Effect of Interfacial Interaction on the Crystallization and Mechanical Properties of PP/Nano-CaCO$_3$ Composites Modified by Compatibilizers

Yuhai Wang, Hao Shen, Gu Li, Kancheng Mai

Key Laboratory of Polymeric Composites and Functional Materials, The Ministry of Education, Materials Science Institute, School of Chemistry and Chemical Engineering, Sun Yat-sen University, Guangzhou 510275, People's Republic of China

ABSTRACT: To investigate the effect of interfacial interaction on the crystallization and mechanical properties of polypropylene (PP)/nano-CaCO$_3$ composites, three kinds of compatibilizers [PP grafted with maleic anhydride (PP-g-MA), ethylene–octene copolymer grafted with MA (POE-g-MA), and ethylene–vinyl acetate copolymer grafted with MA (EVA-g-MA)] with the same polar groups (MA) but different backbones were used as compatibilizers to obtain various interfacial interactions among nano-CaCO$_3$, compatibilizer, and PP. The results indicated that compatibilizers encapsulated nano-CaCO$_3$ particles, forming a core–shell structure, and two interfaces were obtained in the compatibilized composites: interface between PP and compatibilizer and interface between compatibilizer and nano-CaCO$_3$ particles. The crystallization and mechanical properties of PP/nano-CaCO$_3$ composites were dependent on the interfacial interactions of these two interfaces, especially the interfacial interaction between PP and compatibilizer. The good compatibility between PP chain in PP-g-MA and PP matrix improved the dispersion of nano-CaCO$_3$ particles, favored the nucleation effect of nano-CaCO$_3$, increased the tensile strength and modulus, but reduced the ductility and impact strength of composites. The partial compatibility between POE in POE-g-MA and PP matrix had little effect on crystallization and mechanical properties of PP/nano-CaCO$_3$ composites. The poor compatibility between EVA in EVA-g-MA and PP matrix retarded the nucleation effect of nano-CaCO$_3$, and reduced the tensile strength, modulus, and impact strength. © 2009 Wiley Periodicals, Inc. J Appl Polym Sci 113: 1584–1592, 2009

Key words: polypropylene; composites; interfacial interaction; crystallization; mechanical properties

INTRODUCTION

Polypropylene (PP) is one of the most widely used commercial polymers. However, its utilization has been limited because of its poor impact strength and relatively low service temperature. One of the conventional methods for increasing its impact strength is blending with elastomers. However, addition of elastomers generally decreases the yield strength and Young's modulus of PP. In recent years, the use of rigid particles as toughening agents has been proposed.[1] There are a few reports of an increase in toughness of PP upon the addition of rigid particles. Of these rigid particles, calcium carbonate (CaCO$_3$) is most commonly used mainly for its availability in readily usable form and low cost. Therefore, The PP composites filled by micro- and nano-CaCO$_3$ (CC) have been extensively studied.[2–16] Compared to PP/micro-CaCO$_3$ composites, PP/CC composites have attracted considerable interests, because it is believed that the tremendous interfacial area between the filler and the polymer helps to influence the composite's properties to a great extent. Yang et al.[5] demonstrated that CC particles had better toughening effect on improving the impact strength of PP matrix than micro-CaCO$_3$ particles. Chan et al.[7] also found that CC particle was a very effective nucleating agent for PP and significantly increased the impact strength of PP. The toughening mechanism was similar to the rubber-toughening mechanism.[8]

However, rigid particles, especially nanoparticles, usually agglomerate in the polymer matrix due to the tremendous surface area and high surface free energy. Aggregation has a detrimental effect on the properties of polymer composites.[3,8] Therefore, surface treatment is often needed to improve the dispersion of the nanoparticles. The conventional

surface treatment is coating the particles with an organic compound such as stearic acid and titanate coupling agents. Macromolecular compatibilizers[9–11] and irradiation-induced graft polymerization[12] are also used to modify the surface of the particles.

Surface treatment changes the interfacial interaction between $CaCO_3$ particles and PP matrix, and then influences the crystallization behaviors of PP. The $CaCO_3$ particles treated by stearic acid decreased the heterogeneous nucleation for PP crystallization due to the change of the interfacial interaction between PP and $CaCO_3$ particles.[13] Macromolecular compatibilizers enhanced the nucleation ability of $CaCO_3$ particles by improving the interfacial interaction between $CaCO_3$ particles and PP.[9,11] Wang et al.[10] suggested that there existed a synergism of heterogeneous nucleation of CC and macromolecular compatibilizers on the crystallization of PP.

The interfacial interaction also plays an important role in determining the mechanical properties of $PP/CaCO_3$ composites. The modulus and tensile strength of $PP/CaCO_3$ composites decreased by stearic acid treatment[13] but increased when treated with zirconate coupling agent and silane coupling agents.[14] Mai et al.[4] found that the addition of a nonionic modifier greatly improved the Izod impact energy of $PP/CaCO_3$ nanocomposites due to lowering of the particle–polymer interaction. Surface treatment with stearic acid was also favorable for the toughness of $PP/CaCO_3$ composites.[13] It was demonstrated[3,8] that weak interfacial adhesion favored the increase of toughness because it facilitated the debonding of rigid particles, and debonding allowed the plastic deformation of polymer ligaments between the debonded particles. Ma et al.[12] demonstrated that an obvious synergistic effect between the grafted poly(butyl acrylate) (PBA) and CC led to a significant increment in notched impact strength because of the chemical bonding between the elastomer-grafted PBA and CC. However, an opposite result was obtained by Zhang et al.,[15] showing that the encapsulation structure of the filler by the grafting elastomer had a detrimental effect on the impact properties because of the strong adhesion between the elastomer and $CaCO_3$ particle.

A number of investigations indicate that the interfacial interaction significantly influence the crystallization and mechanical properties of $PP/CaCO_3$ composites. For the PP/CC composites modified by compatibilizers with polar group, a core–shell structure is generally formed and there exist two interfacial interactions among CC, compatibilizer and PP: the interfacial interaction between PP and compatibilizer and the interfacial interaction between CC and compatibilizer. Up to now, the effect of interfacial interaction between PP and compatibilizer on the crystallization and mechanical properties of PP/CC composites was rarely reported. In order to investigate the effect of interfacial interaction on the crystallization and mechanical properties of PP/CC composites, three kinds of compatibilizers [PP grafted with maleic anhydride (PP-g-MA), ethylene–octene copolymer grafted with MA (POE-g-MA), and ethylene–vinyl acetate copolymer grafted with MA (EVA-g-MA)] with the same polar groups (MA) but different backbones were used as compatibilizers to obtain various interfacial interactions. It is believed that the MA polar group of compatibilizers would associate with the surface of CC particles by polarity–polarity interaction, resulting in the formation of the core–shell structure in the composites and the formation of the similar interfacial interaction between CC particles and compatibilizers. The different compatibility between the macromolecular chain of compatibilizer and PP matrix results in the formation of different interfacial interaction between PP matrix and compatibilizer. In this article, the effect of the interfacial interaction between PP matrix and compatibilizer on the crystallization behavior and mechanical properties of PP/CC composites was investigated.

EXPERIMENTAL

Materials

Polypropylene (EPS30R), ethylene content 2.87%, MFI = 2.1 g/10 min (2.16 kg at 230°C), T_c= 113.6°C, was supplied by Dushanzi Petroleum Chemical, China. Polypropylene grafted with maleic anhydride (PP-g-MA), grafting ratio 1.0%, MFI > 15 g/10 min (2.16 kg at 230°C), T_c= 113.6°C; Ethylene–octene copolymer grafted with MA (POE-g-MA), grafting ratio 1.1%, MFI = 0.72 g/10 min (2.16 kg at 230°C), T_c = 43.3°C; Ethylene–vinyl acetate copolymer grafted with MA (EVA-g-MA), grafting ratio 1.0%, MFI = 2.46 g/10 min (2.16 kg at 230°C), T_c = 70.2 °C. The compatibilizers were provided by Guangzhou Lushan Chemical Materials Co. China. Nano-$CaCO_3$ (CC), with particle size: 70–90 nm was obtained from Shiraishi Kogyo Kaisha Ltd., Japan.

Sample preparation

All materials were dried in an oven at 60°C for 12 h. PP/CC composites with and without compatibilizers were prepared using a Berstoff ZE25A corotating twin-screw extruder. The blending temperature was set at 200°C. All the materials were simultaneously added into the extruder after previous mixing. The components were in weight ratio. After compounding, the blends were injection molded into rectangular specimens (80 × 10 × 4 mm^3) using a Y-350 vertical injection molding machine at 200°C. A single-edge V-shaped notch of 2 mm depth was milled in the molded specimens for the notched Charpy impact experiments.
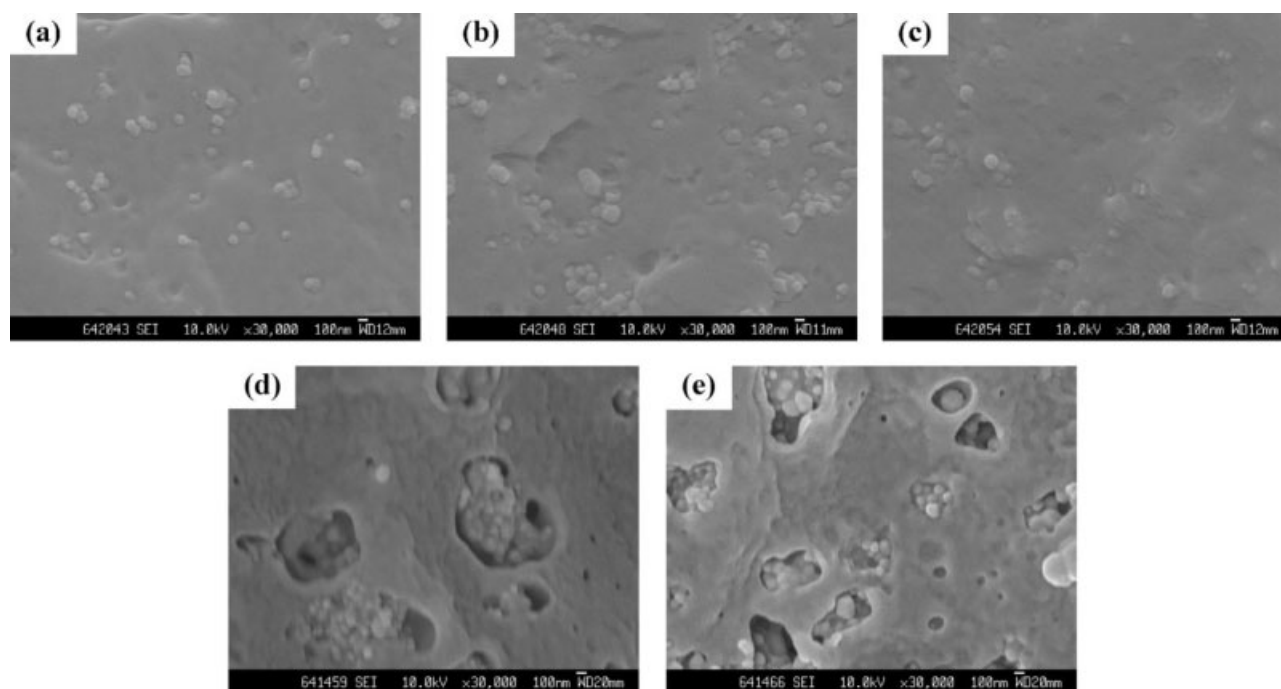
Figure 1 SEM cryofractographs of PP/CC composites with and without compatibilizers: (a) PP/CC(90/10); (b) PP/CC(80/20); (c) PP/PP-*g*-MA/CC (70/10/20); (d) PP/POE-*g*-MA/CC (70/10/20); and (e) PP/EVA-*g*-MA/CC (70/10/20).

Characterization of the composites

The surface tension of PP, compatibilizers, and CC particles was measured at room temperature using a Kruss model K12 contact angle meter. The single liquid method using water and methylene iodide as reference liquids was employed. The dispersion and polar components of the materials were estimated from the contact angle data according to method described in the literature.[17] The surface tension of polymers and CC particles was the sum of dispersion and polar components.

The crystallization behavior of composites was examined using differential scanning calorimetry (DSC) (Perkin–Elmer DSC-7) under nitrogen atmosphere with heating and cooling rates of 10°C/min. The samples were heated from 50 to 220°C, held at that temperature for 3 min, and then cooled to 50°C, followed by reheating to 220°C for the second heating run. The crystallization and melting parameters were recorded from the cooling and reheating scans.

A Rigaku D/max-2200 VPC X-ray diffractometer with the Cu Kα radiation at a voltage of 40 kV and a current of 30 mA was used for wide angle X-ray diffraction (WAXD) experiments. The scan speed was 4°/min in a range of 2θ = 5–40° at ambient temperature. The samples were pretreated on Perkin-Elmer DSC-7 thermal system, heating from 50 to 220°C, holding for 3 min, and then cooling to 50 °C.

The spherulitic morphology of the specimens was observed on ~10-μm thick films cut perpendicularly to the injection molding direction of the rectangular bars with a LEIT2, Orthoplan Pol polarized optical microscope (POM) equipped with a crossed polarizer and a hot stage. The film sample was annealed at 200°C for 3 min via the hot stage, and then the sample was cooled down to room temperature at a rate of 10 °C/min.

Tensile properties were measured using a CMT6103 machine in accordance with GB/T16421-1996. The crosshead speed was set at 50 mm/min. The tensile modulus of the samples was determined at 0.5% strain. Charpy impact strength was obtained from notched specimens, using a JJ-20 impact tester. An impact velocity of 2.9 m/s was used. All mechanical testing was done at room temperature.

The dispersion of CC particles and the morphology of fracture surfaces of Charpy and tensile specimens were examined using a JSM-6330F field emission scanning electron microscope (SEM). The accelerating voltage was set at 10 kV. To obtain a survey of filler dispersion, cryofracturing surfaces of the PP/CC composites obtained at liquid nitrogen temperature were examined. To evaluate the phase morphology of the composites modified by compatibilizers, the cryofractured surfaces were etched with hot heptane for 5 min to remove the elastomer particles from the composite, thus improving contrast between the PP matrix and elastomer phases.

RESULTS AND DISCUSSION

Dispersion of nanoparticles and phase morphology of PP/CC composites

Figure 1 shows the fractured surfaces of PP/CC composites. The dark holes represent the elastomer

TABLE I
The Surface Tension and Its Dispersion, and Polar Component of Materials

Material	Surface tension (mJ/m²)		
	Total (γ)	Disperse component (γ^d)	Polar component (γ^p)
PP	21.0	19.8	1.2
PP-*g*-MA	25.9	23.3	2.6
POE-*g*-MA	29.8	26.7	3.1
EVA-*g*-MA	31.9	26.6	5.3
CC	44.6	16.6	28.0

droplets that were etched by selective solvent. CC particles have a good dispersion at the content of 10 wt %. Most of particles disperse solely in the matrix [Fig. 1(a)]. The size of CC particle is about 70–90 nm. However, CC particles tend to aggregate in the PP matrix with increasing the particles content. Aggregates with sizes of 200–300 nm are observed in the PP matrix when at the content of 20 wt % [Fig. 1(b)]. Compared to the unmodified PP/CC composites, addition of PP-*g*-MA significantly improves the dispersion of CC particles in the PP matrix [Fig. 1(c)]. On the other hand, aggregates with sizes of 1–2 μm in the PP matrix are observed in the PP/CC composites modified by POE-*g*-MA or by EVA-*g*-MA. Compared to PP/CC composite, the interface between PP and CC particles in PP/PP-*g*-MA/CC composite is blurry. For PP/POE-*g*-MA/CC and PP/EVA-*g*-MA/CC composites, the voids around the CC particles are observed because of the absence of compatibilizer etched by selective solvent. Therefore, it is suggested that CC particles are covered with compatibilizer and an encapsulation structure is formed in the PP/CC composites modified by compatibilizers.

In order to analyze the dispersion of CaCO₃ particles and phase morphology of PP/compatibilizer/CC composites, surface characteristic of each component was studied. Table I shows the surface tensions including its dispersion and polar components of all components. The surface tension and polar component of CC particles are markedly higher than those of PP and compatibilizers. The distinct difference in the surface tension and polarity between CC particles and PP will lead to the aggregation of CC particles in PP matrix. On the other hand, because of the higher surface tension of compatibilizers, the ability of compatibilizers to encapsulate CC particles is greater than that of PP. Thus, a core–shell structure is formed in PP/compatibilizer/CC composites. There exists a compatibilizer interphase between CaCO₃ particles and PP matrix and two interfaces formed in the composites: interface between compatibilizer and CC particles and interface between PP and compatibilizer.

The compatibilizers can promote the breakup of agglomerates of CC particles during extrusion process by reducing the particle–particle interaction. However, the dispersion of CC particles in the PP matrix mainly depends on the compatibility between PP and the long hydrocarbon chain in compatibilizer. The increased compatibility between PP and compatibilizer would facilitate the dispersion of CC particles in PP matrix. For PP/CC composite modified by PP-*g*-MA, the good compatibility between PP chain in PP-*g*-MA and PP matrix improves the dispersion of CC particles. For PP/CC composites modified by POE-*g*-MA or EVA-*g*-MA, the poor compatibility of compatibilizers with PP matrix leads the occurrence of subinclusions of CaCO₃ particles into compatibilizer nodules, forming even larger agglomerates of core–shell inclusions.

To evaluate the interfacial interaction of the composites, the interfacial tension and thermodynamic work of adhesion were studied, which can be calculated from the surface tension of the components using the following formulas[16]:

$$\gamma_{AB} = \gamma_A + \gamma_B - 2(\gamma_A^d \gamma_B^d)^{1/2} - 2(\gamma_A^p \gamma_B^p)^{1/2} \quad (1)$$

$$W_{AB} = 2(\gamma_A^d \gamma_B^d)^{1/2} + 2(\gamma_A^p \gamma_B^p)^{1/2} \quad (2)$$

where γ_{AB} is the interfacial tension between phase A and B, W_{AB} is the thermodynamic work of adhesion between phase A and B. γ_A and γ_B are the surface tensions of phase A and B, respectively, and γ^d and γ^p are the dispersion and polar components, respectively.

The calculated interfacial tensions and work of adhesion of all interfaces are shown in Table II. It can be observed that the interfacial tension of PP/CC is high and the work of adhesion of PP/CC is low. This reveals a weak interfacial interaction between PP and CC particles. For the different compatibilizer, the interfacial tension is PP-*g*-MA/CC > POE-*g*-

TABLE II
The Value of Interfacial Tension (γ_{AB}) and Work of Adhesion (W_{AB}) for PP/compatibilizer/CC Composites

Composites	Interfaces	Interfacial tension (γ_{AB}) (mJ/m²)	Work of adhesion (W_{AB}) (mJ/m²)
PP/PP-*g*-MA/CC	PP/PP-*g*-MA	0.39	46.5
	PP/CC	17.4	47.9
	PP-*g*-MA/CC	14.0	56.3
PP/POE-*g*-MA/CC	PP/POE-*g*-MA	0.92	49.8
	PP/CC	17.4	47.9
	POE-*g*-MA/CC	13.4	60.6
PP/EVA-*g*-MA/CC	PP/EVA-*g*-MA	1.93	51.0
	PP/CC	17.4	47.9
	EVA-*g*-MA/CC	9.94	66.3

TABLE III
DSC Results of Neat PP and PP/CC Composites with
and without Compatibilizers

Sample	T_m (°C)	T_c (°C)	$T_m - T_c$ (°C)	ΔH_c (J·g^{-1})
PP	163.7	114.8	48.9	84.1
PP/CC (90/10)	164.4	118.8	45.6	86.6
PP/PP-*g*-MA/CC (85/5/10)	165.5	123.0	42.5	86.1
PP/POE-*g*-MA/CC (85/5/10)	164.7	119.9	44.8	87.5
PP/EVA-*g*-MA/CC (85/5/10)	163.6	114.1	49.5	84.0

T_c, the peak temperature of crystallization; ΔH_c, the heat of crystallization; T_m, the peak temperature of melting.

MA/CC > EVA-*g*-MA/CC and PP/EVA-*g*-MA > PP/POE-*g*-MA > PP/PP-*g*-MA. The work of adhesion is EVA-*g*-MA/CC > POE-*g*-MA/CC > PP-*g*-MA/CC > PP/compatibilizer. The high work of adhesion indicates a strong interfacial adhesion. Therefore, it is suggested that the interfacial adhesion between compatibilizer and CC is stronger than that between PP and CC, and the interfacial adhesion between EVA-*g*-MA and CC is the strongest. However, the high interfacial tension between PP and EVA-*g*-MA due to the distinct difference in polarity would result in a poor compatibility between PP and EVA-*g*-MA. In PP/EVA-*g*-MA/CC composite, a phase separation may occur in the interface between EVA-*g*-MA and PP matrix because of the poor compatibility. On the other hand, in PP/PP-*g*-MA/CC composite, the interface between PP-*g*-MA and PP matrix will be blurry because of the full entanglement of the PP chain. POE-*g*-MA is partial miscible with PP matrix; hence, the interfacial interaction of PP/compatibilizer is PP/PP-*g*-MA > PP/POE-*g*-MA > PP/EVA-*g*-MA.

Crystallization behavior of PP/CC composites

The crystallization behavior and morphology of PP in PP/CC composites are also dependent on the compatibility between PP and compatibilizers. Previous investigation[10] indicated that compatibilizers had little effect on the crystallization behavior of PP matrix. Table III gives a summary of the crystallization and melting data of PP and its composites. Addition of CC particles increases the crystallization temperature of PP due to the heterogeneous nucleation of CC particle. The crystallization temperature of PP in PP/PP-*g*-MA/CC composite is approximately 8°C higher than that of neat PP and 4°C higher than that of PP/CC composite. It is suggested that there exists a synergism of heterogeneous nucleation of PP-*g*-MA and CC particles for PP crystalli-

zation. The application of POE-*g*-MA slightly increases the crystallization temperature of PP in PP/CC composite. However, the addition of EVA-*g*-MA significantly decreases the crystallization temperature of PP in PP/CC composite. Addition of CC particles and compatibilizers has little influence on the crystallinity.

Figure 2 shows the WAXD patterns of neat PP and its composites with and without compatibilizers. For the PP/CC composites modified by PP-*g*-MA or by POE-*g*-MA, except for the characteristic crystalline peaks of α-crystal of PP, a peak at 2θ≈16° corresponding to β-crystal of PP is observed. There are no crystalline peaks of β-crystal of PP in neat PP, PP/CC composite, and its composite modified by EVA-*g*-MA. It is suggested that the formation of β-crystal of PP is induced by the synergistic effect of CC particle and compatibilizer, but it also depends on the compatibility between PP matrix and compatibilizer.

Figure 3 shows the optical micrographs of neat PP and its composites. The spherulite size of neat PP is larger than 100 μm, and the interfaces among the spherulites are sharp and clear [Fig. 3(a)]. Addition of CC particles dramatically increases the number of spherulites and decreases the size of spherulites because of the heterogeneous nucleation of CC particles [Fig. 3(b)]. Addition of PP-*g*-MA further decreases the size of PP spherulites because of the synergism of heterogeneous nucleation of PP-*g*-MA and CC particles [Fig. 3(c)]. The spherulites are too small to be detected in this micrograph. Addition of POE-*g*-MA has little effect on the spherulites morphology of PP in PP/CC composite [Fig. 3(d)]. However, the spherulite size of PP in PP/EVA-*g*-MA/CC composites is larger than that of PP/CC composite
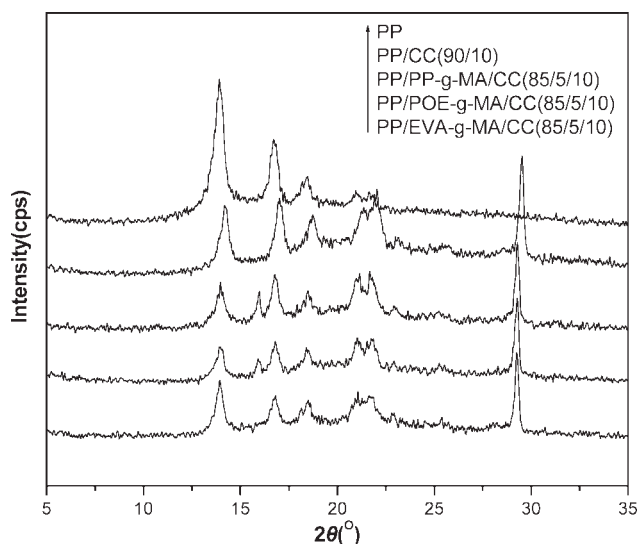
Figure 2 WAXD patterns of neat PP and PP/CC composites with and without compatibilizers.
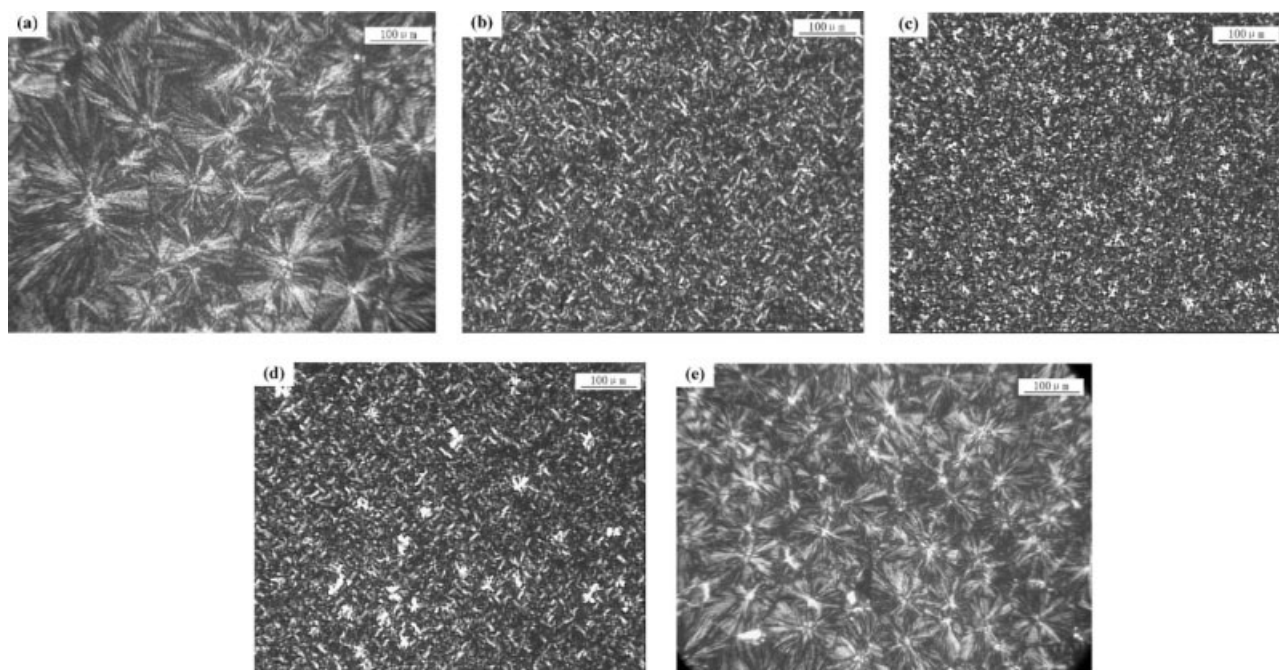
Figure 3 Optical micrographs of spherulite textures: (a) PP; (b) PP/CC (90/10); (c) PP/PP-*g*-MA/CC (85/5/10); (d) PP/POE-*g*-MA/CC (85/5/10); and (e) PP/EVA-*g*-MA/CC (85/5/10).

[Fig. 3(e)]. It is suggested that addition of EVA-*g*-MA retards the heterogeneous nucleation of CC particles.

The polar groups (MA) of compatibilizers may react with CC particles by chemical bond and lead to the formation of carboxylate salts, just as demonstrated by Tabtiang and Venables.[18] Compared to CC particles, the carboxylate salts can act as a more effective nucleating agent, further increasing the crystallization temperature of PP and induces the formation of β-crystal of PP. However, the carboxylate salts are localized in the interface between $CaCO_3$ particles and the compatibilizer. They do not play a direct nucleation effect for PP matrix because of the presence of the compatibilizer layer and may first nucleate the compatibilizer layer or the PP matrix chains included in this layer, and then nucleate the PP matrix. Therefore, the nucleation by carboxylate salts depends on the compatibility between PP and compatibilizer and on the crystallization capacity of compatibilizer. Characterization of the compatibilizer indicates that the crystallization temperature of PP-*g*-MA is close to that of PP matrix and the crystallization temperatures of POE-*g*-MA and EVA-*g*-MA are much lower than that of PP matrix. Therefore, for the composite modified by PP-*g*-MA, the carboxylate salts can nucleate the PP-*g*-MA layer which, in turn, nucleates the PP matrix by secondary nucleation through the completely miscible interface layer. For the composites modified by POE-*g*-MA or by EVA-*g*-MA, the crystallization of these two compatibilizers does not affect the crystalliza-

tion of PP matrix because of their lower crystallization temperatures. Thus, the nucleation by carboxylate salts depends on the compatibility between PP matrix and compatibilizer in these two modified composites. For the composite modified by POE-*g*-MA, the PP and POE chains in POE-*g*-MA is partial miscible. The partial miscible interface layer weakens the nucleation effect of carboxylate salts. For the composite modified by EVA-*g*-MA, the incompatibility between PP and EVA-*g*-MA and noncrystalline of EVA retard the nucleation by carboxylate salts.

Tensile properties and fracture morphology of PP/CC composites

Table IV gives a summary of tensile properties of composites. The Young's modulus gradually increases but the yield strength decreases with increasing $CaCO_3$ content. The elongation at break shows a maximum at 5 wt % of $CaCO_3$ but decreases remarkably with increasing $CaCO_3$ content. Addition of PP-*g*-MA increases both the Young's modulus and the yield strength, but decreases the elongation at break. Addition of POE-*g*-MA slightly reduces both Young's modulus and yield strength. On the other hand, EVA-*g*-MA significantly decreases both Young's modulus and yield strength, but recovers the elongation at break.

During the tensile process, CC particles act as stress concentrators and produce high tensile stress around the particles because of the large differences

Mechanical Properties of PP and PP/CC Composites with and without Compatibilizers

Composites	Tensile modulus (GPa)	Tensile strength (MPa)	Elongation at break (%)	Impact strength (kJ/m^2)
PP	0.65 ± 0.02	34.0 ± 0.4	99.8 ± 9.5	4.40 ± 0.41
PP/CC (95/5)	0.71 ± 0.01	32.2 ± 0.2	173.6 ± 21.0	6.41 ± 0.69
PP/CC (90/10)	0.78 ± 0.02	34.1 ± 0.6	72.7 ± 4.0	23.80 ± 0.27
PP/CC (85/15)	0.78 ± 0.02	30.8 ± 0.6	89.9 ± 7.9	22.10 ± 1.09
PP/CC (80/20)	0.80 ± 0.01	30.6 ± 0.3	74.6 ± 6.3	20.70 ± 0.80
PP/PP-g-MA/CC (85/5/10)	0.85 ± 0.03	36.0 ± 0.6	65.8 ± 3.5	3.98 ± 0.49
PP/POE-g-MA/CC (85/5/10)	0.74 ± 0.01	33.9 ± 0.5	73.6 ± 3.5	25.99 ± 0.68
PP/EVA-g-MA/CC (85/5/10)	0.66 ± 0.02	32.5 ± 1.2	84.7 ± 8.4	3.86 ± 0.20

in elastic properties between CC particles and PP matrix.[8] Because the interfacial adhesion between CC particles and PP matrix is weak, the debonding will take place at the interface and leads to a lowering of the yield strength. On the other hand, the interface between particle and PP does not debond at low strain, so addition of CC increases the modulus of composite due to the high modulus of rigid particle.

As discussed in "Dispersion of Nanoparticles and Phase Morphology of PP/CC Composites" section, the interfacial adhesion of compatibilizer/CC is larger than that of PP/compatibilizer. During tensile process, the debonding will take place at the interface between PP and compatibilizer prior to the interface between compatibilizer and particle. Thus, the mechanical properties of PP/CC composite are mainly dependent on the interface interaction between PP and compatibilizer. For PP/PP-g-MA/CC composite, the good compatibility between PP-g-MA and PP matrix results in a strong interfacial adhesion between PP-g-MA and PP. The enhanced interfacial adhesion resists the debonding of the interface between PP-g-MA and PP matrix, and improves the yield strength of the composites. At the same time, the stress can be easily transferred through the interfacial layer between PP-g-MA and PP, leading to a significant increase of modulus. For the PP/CC composite modified by POE-g-MA or by EVA-g-MA, the poor compatibility between compatibilizer and PP matrix results in a weak interfacial adhesion between the compatibilizer and PP matrix. The weak interfacial adhesion facilitates the debonding of the interface between compatibilizer and PP matrix, leading to a reduction of yield strength. The elastomeric layers between CaCO$_3$ and PP matrix suppress the transfer of stress, resulting in a decrease of the modulus. The change of the modulus in PP/compatibilizer/CC composite is also related to the dispersion of CaCO$_3$ particles, and a good dispersion of CaCO$_3$ particles will increase the modulus of the composites.

Figure 4 shows the tensile fracture surfaces of PP/CC composites with and without compatibilizers along the direction of deformation. The fracture
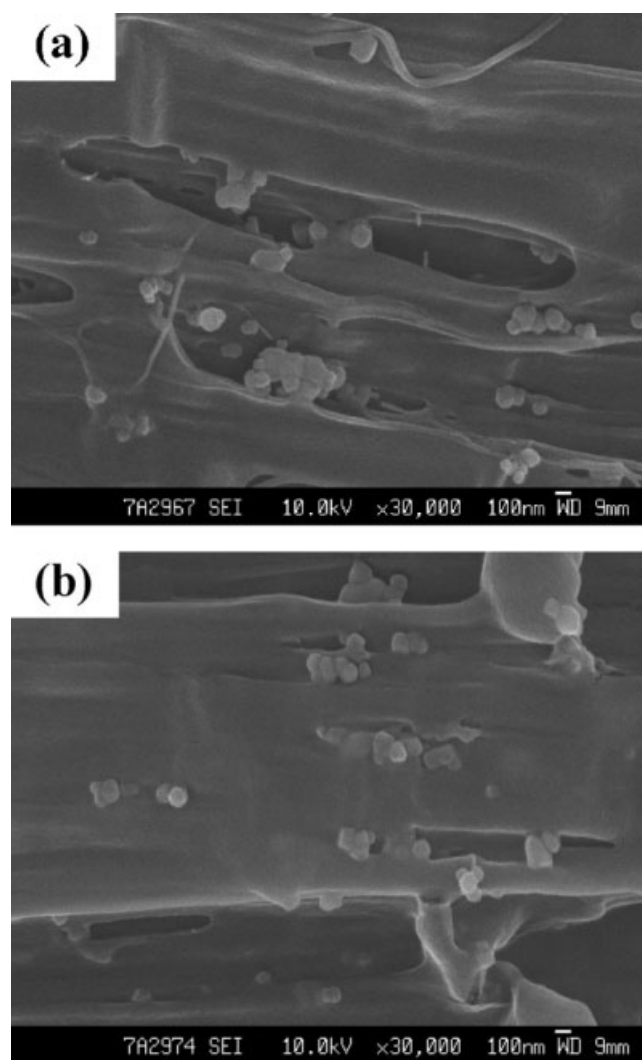
Figure 4 SEM photographs of tensile fracture surfaces of PP/CC composites with and without compatibilizers along the direction of deformation: (a) PP/CC (90/10); (b) PP/PP-g-MA/CC (85/5/10).

surface of PP/CC composite exhibits elongated cavities around the debonded particles, and the matrix ligaments between these cavities are stretched and deformed extensively [Fig. 4(a)]. Cavitation will increase the elongation of the samples. For example, PP/CC (95/5) sample shows an elongation of 173%. However, high CaCO$_3$ content induces early fracture due to the aggregates of CaCO$_3$ particles, the large aggregates may act as sites for fracture initiation during tensile drawing. Figure 4(b) shows that there are not much cavities and extensive deformation on the fracture surface of PP/CC composite modified by PP-g-MA. The CC particles cling tightly to the matrix and rarely debond. This confirms the hypothesis that a strong interfacial adhesion between compatibilizer and PP matrix resists the debonding of CaCO$_3$ particles.

Charpy impact property and fracture morphology of PP/CC composites

The notched Charpy impact energies of neat PP and PP/CC composites with or without the compatibilizers are given in Table IV. Neat PP is brittle with the notched impact strength of only 4.4 kJ/m^2. The incorporation of CC particles significantly increases the impact strength of PP and displays a maximum of 23.8 kJ/m^2 at 10 wt % CaCO$_3$. The impact strength of PP/CC composites decreases with increasing filler loading, but it still reaches a value of 20.7 kJ/m^2 at 20 wt % CaCO$_3$, which is about five times that of neat PP.

Addition of compatibilizers has a great effect on the impact strength of PP/CC composites. Addition of POE-g-MA further increases the impact strength. However, the incorporation of PP-g-MA or EVA-g-MA is detrimental to the impact strength. The PP/CC composites modified by PP-g-MA or EVA-g-MA show impact strengths of 3.98 and 3.86 kJ/m^2, respectively, which are even lower than the one of neat PP.

SEM micrographs of impact-fractured surfaces of neat PP and PP/CC (90/10) composite are showed in Figure 5. Neat PP exhibits a brittle failure characteristic at room temperature [Fig. 5(a)]. Incorporation of CaCO$_3$ particles into PP causes extensive plastic deformation on the fracture surface [Fig. 5(b)]. The PP/POE-g-MA/CC composite, with high impact strength, exhibits a similar fracture surface of PP/CC composite. However, the composites modified by PP-g-MA or EVA-g-MA, which have low impact strength, show rather flat fracture surfaces as neat PP.

The toughening mechanism of rigid particles consists of three stages: stress concentration, debonding, and shear yielding.[8] In the PP/CC composites, the CaCO$_3$ particles, which act as stress concentrators
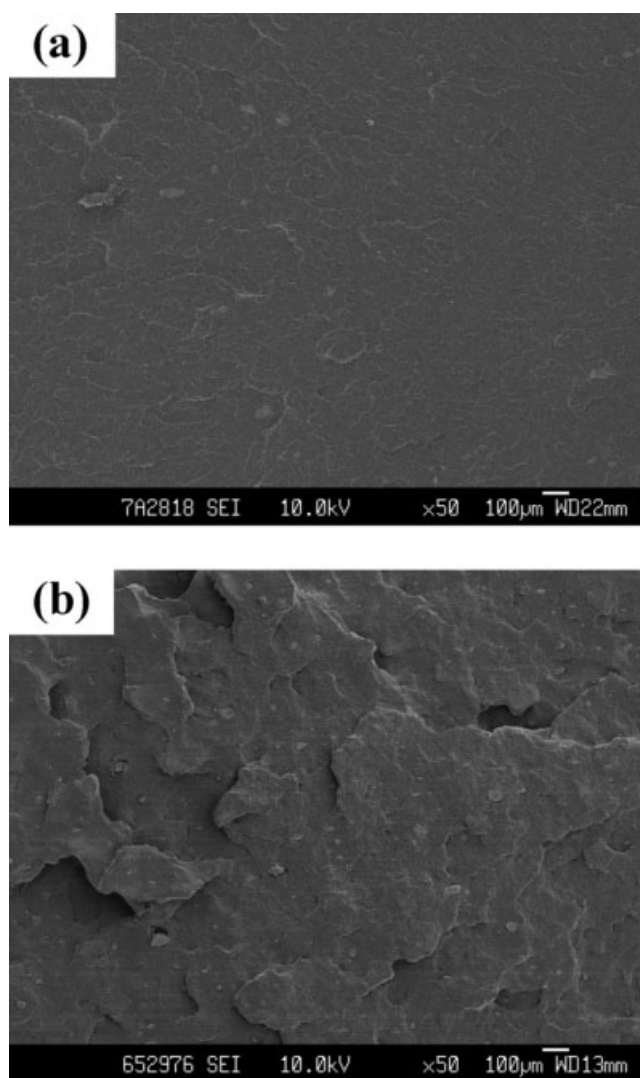
Figure 5 SEM micrographs of impact-fractured surfaces: (a) neat PP; (b) PP/CC (90/10).

during impact process, leads to the debonding of CaCO$_3$ particles, resulting in high impact toughness.

The interfacial adhesion and interaction between particle and matrix play an important role in the debonding mechanisms during fracture process. Strong adhesion may retard the debonding among interfaces and lead to a low toughness. Contrary, low interfacial adhesion facilitates debonding and as a result favors toughness. Vollengberg and Heikens[19] reported a decrease of impact strength in chalk-filled PP composites because of strong interfacial bonding. Mai et al.[4] also found that a weak filler–matrix interface was favorable for toughness enhancement.

The low impact strength of PP/PP-g-MA/CC composite is attributed to the strong interfacial adhesion between PP-g-MA and PP, which resists the debonding among the interfaces. The high fracture toughness of PP/CC composite and PP/POE-g-MA/CC

composite is attributed to the weak interfacial adhesion between PP and CC and between PP and POE-g-MA, which allows the debonding among the interfaces. However, PP/EVA-g-MA/CC composite, which is expected to have high fracture toughness because of the toughness effect of EVA and the easy debonding of the interface of PP/compatibilizer because of the low interfacial adhesion, shows low impact strength. The reason likely corresponds to the suggestions proposed by Premphet and Horanont[20] and Zhang et al.[15] It was believed that cracks could easily propagate along the interface during impact fracture because of the poor interfacial adhesion between PP and EVA, resulting in the poor impact strength.[20] Zhang et al.[15] also suggested that one of the reasons for the lower toughness caused by core–shell structure might be that the restriction effect of the cavitation and elongation of the elastomer caused the strong interfacial interaction between the elastomer and the filler. Thus, much further work is necessary to unfold the effect of interfacial interaction on the toughness mechanisms of PP/compatibilizer/CC composites.

CONCLUSIONS

In PP/CC composites modified by compatibilizer, the compatibilizers encapsulated CC particles, resulting in the formation of a core–shell structure. There exists a compatibilizer interphase between $CaCO_3$ particles and PP matrix and two interfaces in the compatibilized composites: interface between PP and compatibilizer and interface between compatibilizer and CC particles. The crystallization and mechanical properties of PP/CC composites were dependent on the interfacial interactions of these two interfaces, especially the interfacial interaction between PP and compatibilizer. The surface tension results demonstrated that the interfacial interaction between compatibilizer and CC is higher than those between PP and CC, and between compatibilizer and PP. DSC results showed that there existed a synergism of heterogeneous nucleation of the polar groups (MA) of compatibilizers and CC on the crystallization of PP, but the synergism of heterogeneous nucleation was affected by the compatibility between PP matrix and compatibilizer. The good compatibility between PP-g-MA and PP matrix improved the dispersion of CC particles, favored the nucleation effect of CC, increased the tensile strength and modulus but reduced the ductility and impact strength of composites. The partial compatibility between POE-g-MA and PP matrix had little effect on crystallization and mechanical properties of PP/CC composites. The poor compatibility between EVA-g-MA and PP matrix retarded the nucleation effect of CC, reduced the tensile strength, modulus and impact strength.

References

1. Kim, G. M.; Michler, G. H. Polymer 1998, 39, 5689.
2. Li, G.; Mai, K. C.; Feng, K. C.; Huang, Y. P. Polym Int 2006, 55, 891.
3. Thio, Y. S.; Argon, A. S.; Cohen, R. E.; Weinberg, M. Polymer 2002, 43, 3661.
4. Zhang, Q. X.; Yu, Z. Z.; Xie, X. L.; Mai, Y. W. Polymer 2004, 45, 5985.
5. Yang, K.; Yang, Q.; Li, G. X.; Sun, Y. J.; Feng, D. C. Polym Compos 2006, 27, 443.
6. Akovali, G.; Akmant, M. A. Polym Int 1997, 42, 195.
7. Chan, C. M.; Wu, J. S.; Li, J. X.; Cheung, Y. K. Polymer 2002, 43, 2981.
8. Zuiderduin, W. C. J.; Westzaan, C.; Huetink, J.; Gaymans, R. J. Polymer 2003, 44, 261.
9. Avella, M.; Cosco, S.; Di, Lorenzo, M. L.; Di, Pace, E.; Errico, M. E. J Therm Anal Calorim 2005, 80, 131.
10. Wang, Y. H.; Shen, H.; Mai, K. C. Acta Materiae Compositae Sinica 2006, 23, 14.
11. Lin, Z. D.; Huang, Z. Z.; Zhang, Y.; Mai, K. C.; Zeng, H. M. J Appl Polym Sci 2004, 91, 2443.
12. Ma, C. G.; Rong, M. Z.; Zhang, M. Q.; Friedrich, K. Polym Eng Sci 2005, 45, 529.
13. Rungruang, P.; Grady, B. P.; Supaphol, P. Colloids Surf A 2006, 275, 114.
14. Doufnoune, R.; Haddaoui, N.; Riahi, F. Int J Polym Mater 2006, 55, 815.
15. Zhang, L.; Li, C. Z.; Huang, R. J Polym Sci Part B: Polym Phys 2005, 43, 1113.
16. Premphet, K.; Horanont, P. Polymer 2000, 41, 9283.
17. Yang, H.; Zhang, X. Q.; Qu, C.; Li, B.; Zhang, L. J.; Zhang, Q.; Fu, Q. Polymer 2007, 48, 860.
18. Tabtiang, A.; Venables, R. Eur Polym J 2000, 36, 137.
19. Vollenberg, P. H. T.; Heikens, D. J Mater Sci 1990, 25, 3089.
20. Premphet, K.; Horanont, P. J Appl Polym Sci 2000, 76, 1929.